PROCEEDINGS, 50th Workshop on Geothermal Reservoir Engineering
Stanford University, Stanford, California, February 10-12, 2025
SGP-TR-229

Flow and thermal modeling of a geothermal doublet in a layered reservoir of Paris Basin.

Emmanuel Mouche, Maxime Catinat*, Daniel Otoo, Benjamin Brigaud*, and Pascal Audigane**

Laboratoire des Sciences du Climat et de l'Environnement, C.E. de Saclay, Orme des merisiers, 91191 Gif sur Yvette, France

*Université Paris-Saclay, GEOPS, CNRS, 91405 Orsay, France

**Bureau de Recherches Géologiques et Minières, 45060 Orléans, France

Emmanuel.mouche@lsce.ipsl.fr

Keywords: Geothermal Doublet, Modeling, Layered Aquifer, Gringarten and Sauty, Upscaling

ABSTRACT

The Dogger carbonate formation of Paris Basin is a target for geothermal exploitation since the late 1960's. The reservoir consists of a hot water aquifer of regional extent composed of pervious oolithic limestones and dolomites of Mid-Jurassic age. The depths and temperatures are ranging from 1450 to 2000 m and 56 to 80°C respectively. Based on flowmeter logs and seismic surveys the pervious units are conceptualized as layers of large extent, greater than the mean inter-well distance, 10^3 metres, a few metres thick and interbedded by aquitards. The geothermal performance of a doublet is measured by two indicators: the cold-water breakthrough time and the temperature reached in the producer well after thirty years. These indicators are assessed for each doublet by geomodelling and flow and thermal numerical simulation. Another modeling tool of interest for the layered geology of Paris Basin is the model proposed by Gringarten and Sauty in 1975. Their model gives the time evolution of the temperature in a producer well for a single pervious infinite layer embedded into an impervious host rock. This model is very valuable as it links analytically the thermal response of a doublet to the physical parameters of the system. Nevertheless, it cannot be extended to the multilayered case and is of little help to tackle the connectivity issue raised when layers are of finite extent. In this paper we address these two heterogeneity issues by means of geostatistical simulations and upscaling approaches. We propose to keep the Gringarten and Sauty modeling framework and explore how to account for both vertical and lateral heterogeneities by using equivalent parameters.

1. INTRODUCTION

In France, low enthalpy-resources are primarily tapped from the Paris basin. In the basin, the Middle Jurassic (Dogger) carbonate reservoir, located at a depth of about 1.5 km, is identified since the 1980s as the most promising target for the development of geothermal energy (Figure 1(a)) (Antics et al., 2005; Lopez et al., 2010). In Ile-de-France region, fifty-four district heating production units exploit the heat capacity of a deep reservoir at 55-80°C formed by the 175 m thick Bathonian limestones (Figure 1(b)) (Thomas et al., 2023; Catinat et al., 2023a, 2023b). This reservoir is characterized by heterogenous rocks resulting from wide variability of depositional environments and diagenetic processes. The majority of geothermal production is provided by the « Oolithe Blanche » formation which consists of ooid limestones deposited on a high-energy shallow platform (Lopez et al., 2010). In the reservoir, the productive layers identified by regular flowmeter logs interpretations in geothermal wells reveal a heterogeneous vertical structure (Hamm et al., 2015). These layers, averaging 2 m in Ile-de-France, can be interpreted as poro-permeable lenses which appear to extend at least 500 and up to 2000 m within the reservoir (Catinat et al., 2023a, 2023b).

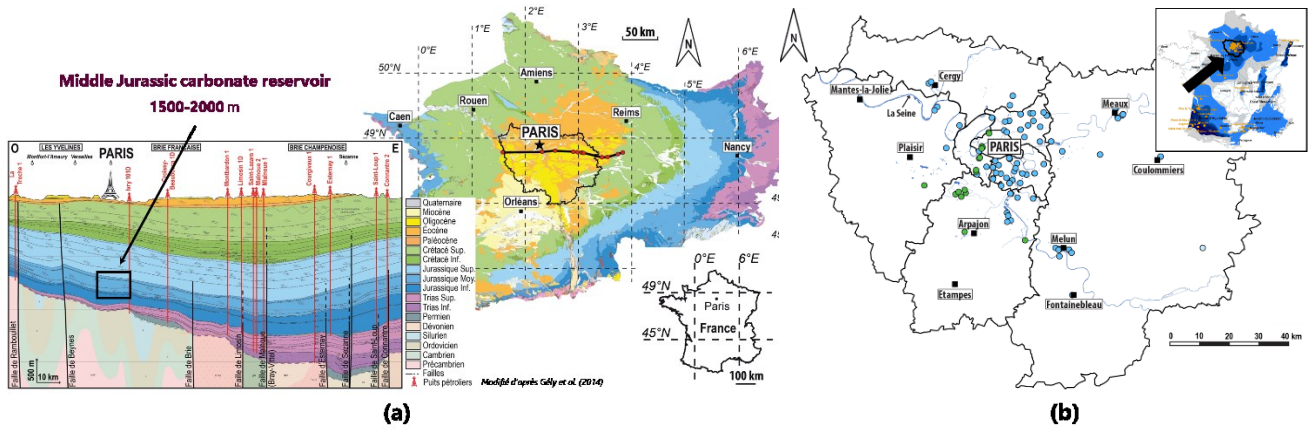

Figure 1: (a) Geological map of the Paris Basin with Ile de France region boundary and a vertical cross section showing the Middle Jurassic geothermal reservoir. (b) Location map showing the geothermal wells in Ile de France region.

These observations led to propose different multilayered models of infinite extent (Figure 2(a)) to simulate the temperature production of a doublet (Antics et al., 2005; Lebrun et al. 2011; Catinat 2023c). These models are conceptually derived from the single layer model developed by Gringarten and Sauty (G&S) (Gringarten and Sauty, 1975). In the single layer approach all the productive sublayers are merged into a single one embedded into the impervious host rock. The impervious sublayers sandwiched between the pervious sublayers are neglected. The upper part of the host rock is called the overburden and the lower one the underburden. In the sandwich model the single productive layer of the monolayer approach is split into two identical layers and the impervious sublayers are merged into a single impervious layer, the aquitard, and sandwiched between the two productive layers (Figure 2(a)). In the multilayered approach the layering, as measured in flow log experiments, is respected. Nevertheless, as the layering observed in the injection and production wells do not generally correspond (Figure 2(b)), two layered models are developed: one model with the layering observed in one well and applied to the other well, and the second model with the inverse procedure. The production temperature is then assumed to be the mean temperature of the two models.

These different models have been integrated in numerical codes over the past two decades (see Catinat, 2023c). If these digitized models help to quantify the impact of each representation scenario on the production temperature they are of little help to understand the physics of thermal transfer between the layers (pervious and impervious) and with the burdens, and also understand the link between the parameters (geometrical and physical) and the production temperature. For this reason, we revisit the classical G&S model and explore how their semi-analytical model may help to solve these issues. Our methodology is based on a comprehensive comparison between results obtained with computer codes and the G&S model or some of its variants.

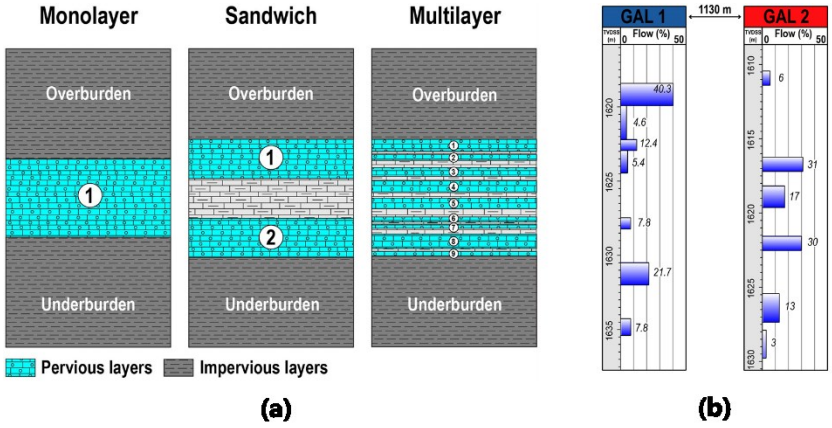

Figure 2: (a) Different schematic representations of the multilayer structure of the Dogger aquifer in Ile de France region. (b) Flow logs in the injection well (GAL1) and production well (GAL2) of the Alfortville doublet.

2. THE MODELS

2.1 Gringarten and Sauty model

In their paper of 1975 Gringarten and Sauty (G&S) give the space and time evolution of the temperature distribution in a dipole flow field in a single pervious infinite 3D horizontal layer of constant thickness and embedded into an impervious host rock. The main assumptions are: i) the temperature across the layer thickness is constant which allows vertical averaging of the water temperature transport equation; ii) the temperature in the cap rock is governed by a 1D heat conduction equation along the vertical; iii) dispersion and diffusion processes in the layer are neglected and the water temperature transport is purely advective. These assumptions lead to heat transport equations:

layer: $$h\rho_a C_a \frac{\partial T_w}{\partial t} + \rho_w C_w Q \frac{\partial T_w}{\partial s} = 2K_r \frac{\partial T_r(z=h/2)}{\partial z} \quad (1)$$

host rock: $$\rho_r C_r \frac{\partial T_r}{\partial t} = K_r \frac{\partial^2 T_r}{\partial z^2} \quad (2)$$

where h is the layer thickness, Q the flowrate, and T_i, $\rho_i C_i$, K_i the temperature, the heat capacity and the thermal conductivity of material i respectively (i=w for water, r for rock, a for aquifer). The streamtube surface, s, links injection and production wells: $s = 0$ at the injection well and $s = s_{max}$ at the producer well. The temperature in the layer T_w is given as an integral over all the streamtubes. Here, we prefer to rewrite the solution as an integral over all the streamlines:

Water temperature: $$T_w(\theta, t) = T_{inj}\, erfc\left[\frac{\tau(\theta)}{(t - t_a(\theta))}\right]^{1/2} \quad (3)$$

Production temperature: $$T_{prod}(t) = \left(1 - \frac{\theta(t)}{\pi}\right) T_{rock} + \frac{1}{\pi}\int_0^{\theta(t)} d\theta'\, T_w(\theta', t) \quad (4)$$

Where θ is the streamline angle at the injection well (Figure 3(a)) and $\theta(t) \equiv \theta\big(t = t_a(\theta)\big)$ is the cumulative arrival time distribution of the particles launched at the injection well and advected along the streamlines. The expressions of the particle arrival time, or breakthrough

time, t_a, and streamline length L distributions with respect to θ are given by Barker (1981). The values of t_a and L for $\theta = 0, \pi/2, 3\pi/4$ are respectively $t_a(0)$, $t_a(\pi/2) = 3t_a(0)$, $t_a(3\pi/4) = 20.13t_a(0)$ and $L(0) = D$, $L(\pi/2) = 1.57D$, $L(3\pi/4) = 3.33D$. From a physical point of view these values mean that at time $t_a(\pi/2)$ the water temperature in the production well accounts for heat transport and heat exchange with the caprock in a circle region centered at the midpoint between the two wells. The temperature plume traveling outside this region has not reached the production well at that time and does not contribute to the production temperature. The characteristic time $\tau(\theta) = \lambda t_a(\theta)$ where λ is a dimensionless parameter that reflects the strength of the thermal coupling between the rock and the layer. For given materials heat capacity and heat conductivity values we have the dependencies: $t_a(0) \sim D^2 h/Q$ and $\lambda \sim Qh/D^2$. The larger the parameter λ, the weaker the coupling. When coupling with host rock (the burdens) is disregarded the production temperature is given by the streamline model: $T_{prod}(t) = (1 - \theta(t)/\pi)T_{rock} + \theta(t)/\pi T_{inj}$

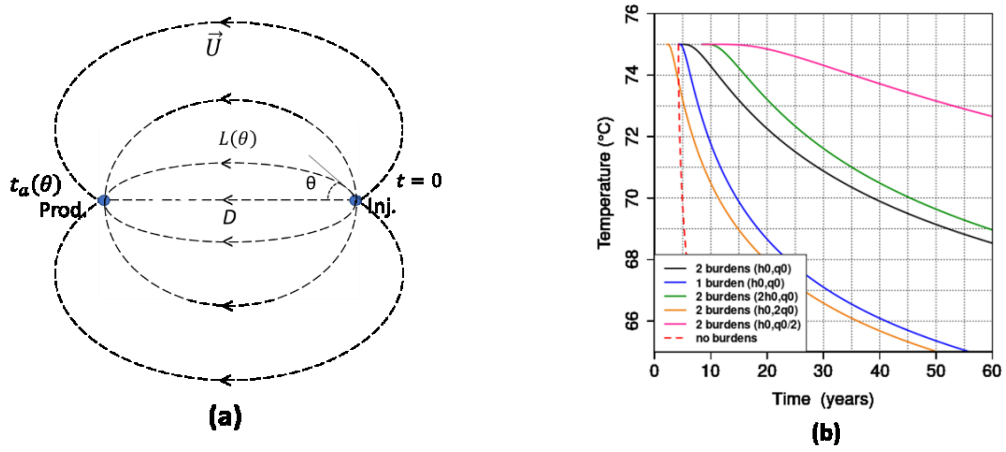

Figure 3: (a) Dipole flow field generated by a doublet. (b) Production temperature given by the streamline model (red dotted curve) and the G&S model (solid curves) for different values of the flowrate Q and permeable layer thickness h (black (Q_0,h_0), green (Q_0,$2h_0$),orange ($2Q_0$,h_0), pink ($Q_0/2$,h_0). The blue dotted curve corresponds to G&S model with heat exchange with the over or underburden only.

Table1: Geometrical and physical parameters of Alfortville doublet.

Geometrical and physical parameters of Alfortville doublet	
Interwell distance	1130 m
Injection flowrate	193 m^3/h
Initial burden temperature	75°C
Injection temperature	49°C
Fluid pressure	170 bars
Fluid salinity	18 g/L
Rock thermal conductivity	2.5 $Wm^{-1}K^{-1}$
Fluid thermal conductivity	0.6 $Wm^{-1}K^{-1}$
Rock heat capacity	2.16 MJ $m^{-3}K^{-1}$
Fluid heat capacity	4.18 MJ $m^{-3}K^{-1}$

Figure 2 (b) display the production temperature given by the streamline model (red dotted curve) and the G&S model (solid colored lines) for the Alfortville doublet (south east of Ile de France) over 60 years. The different physical rock, fluid and flow parameters are given in Table 1 and the nominal pervious layer thickness, h_0, is assumed to be 9.2 m. We see that the breakthrough time t_a ($\equiv t_a(0)$), varies with h and Q according to the ratio h/Q, and its value is 4.35 years for $h=h_0$. For the same λ value (same production temperature) but two different breakthrough times the production curves are very different from each other (green and orange curves). As expected, we observe the importance of the heat supplied by the burdens: no burden (red), one burden (blue) and the two burdens (black).

2.2 Sandwich model

The sandwich model is a schematic conceptualization of a multi layered system: two identical pervious layers with an interbedded impervious layer, the whole embedded in a host rock (Figure 2(a)). There is no analytical solution to this problem. Let us mention that literature on fractured rock gives a semi analytical solution for a periodic system of parallel 1D fractures (Sudicky and Frind, 1982). This

solution is complex and does not have the simplicity of the G&S solution. The equations describing the sandwich system are similar to the equations of the single layer case (Equations (1), (2)). There are two source terms in the water temperature transport equation, one describing heat transfer towards the burdens and the other towards the impervious layer. Let us assume that heat exchange between the two layers (pervious and impervious) is described by a first order kinetic law:

$$\frac{\partial T_{imp}}{\partial t} = \frac{T_w - T_{imp}}{\tau} \tag{5}$$

where τ is a characteristic heat transfer time. As τ may be considered much smaller than the travel time between the two wells t_a the solution may be searched as an expansion in powers of $\varepsilon = \tau/t_a$. At the zeroth order, the impervious and the pervious layers are in thermal equilibrium $T_w = T_{imp}$ and the water temperature in the pervious layer is described by the effective equation:

$$(h\rho_a C_a + e\rho_r C_r)\frac{\partial T_w}{\partial t} + \rho_w C_w Q \frac{\partial T_w}{\partial s} = 2K_r \frac{\partial T_r(z=h/2)}{\partial z} \tag{6}$$

Where e is the thickness of the impervious layer. The heat transfer equation in the caprock remains unchanged. This effective equation means that the effective water velocity and heat transfer towards the caprock are smaller than in the single layer case. If the first order term ε is considered, some diffusion terms appear but the expressions become intricated. Finally, equation 6 is solved as equation 1 in the G&S model, *i.e.* $h\rho_a C_a$ is replaced by $h\rho_a C_a + e\rho_r C_r$. When the burdens are neglected the expressions become simpler and the ε term is a diffusion term which transforms the initial advection equation into an advection-dispersion equation. In this case (no burdens) an exact solution may be found in the literature (see § 15.3 "Heat regenerators and heat exchangers" in Carslaw and Jaeger, 1959). The physics of this type of system, *i.e.* an immobile phase in contact with a moving phase, is studied since long in geosciences (Lauwerier, 1955; Haggerty and Gorelick, 1995).

2.3 Heterogeneous media

In heterogeneous media the permeability varies spatially and the dipole flownet associated to a doublet gives a picture of the permeability field: streamlines converge towards high permeability zones and diverge in low permeability zones. When the permeability variation spans over more than one order of magnitude the streamlines convergence define flow channels. Outside these channels flow is negligible. In 2D the often-cited channeling example is the tracer transport in a single fracture with a varying aperture (Tsang and Tsang, 1989). An example applied to a geothermal doublet in a fracture may be found in (Guo et al., 2016). Another channeling example related to the present work is the percolation through a random distribution of conducting disks embedded into an impervious rock matrix (King, 1990). The disks may be, for example, pervious lenses or fractures. When the density of these geobodies is low, *i.e.* below some percolation threshold, flow cannot take place. The disks connectivity is not high enough. In the opposite case, flow percolation takes place through channels.

The G&S model may be extended to 2D heterogeneous cases under certain assumptions. Equations (1) and (2) remain unchanged, except that the flow rate Q depends now on θ (*i.e.* on the streamtube). The streamline solution given by Equation (3) remain also unchanged. The mixing law (Equation 4) becomes

$$T_{prod}(t) = T_{rock}\frac{1}{Q}\int_{-\pi}^{\pi} d\theta' dQ(\theta') H(t_a(\theta') - t) + \frac{1}{Q}\int_{-\pi}^{\pi} d\theta'\, dQ(\theta') H(t - t_a(\theta')) T_w(\theta', t) \tag{7}$$

Where $dQ(\theta)$ is the flowrate distribution along the injection well boundary and H is the Heaviside function. The flowrate $dQ(\theta)$ and the arrival time $t_a(\theta)$ distributions have to be determined by simulation. As it is the inter-well zone that plays a role in the thirty first years period some simplifying assumptions can be made on these distributions when the heterogeneity scale is of the order of magnitude of the inter-well distance (Mouche et al., in prep.).

3. IMPACT OF THE DISTRIBUTION OF LAYERS

The survey of the Dogger reservoir shows that the pervious layers intercepted by the geothermal wells are not of infinite extent, but larger than the inter-well distance of any doublet, almost parallel at the doublet scale and with varying thicknesses (Lopez et al., 2010; Hamm et al., 2015). Here we assume that the thickness of a given layer is constant but may vary from one layer to another one. This type of layer distribution raises the question of defining an equivalent layer. The issue has been addressed previously by means of numerical simulation (Antics et al., 2005; Lebrun et al., 2010) on distributions of parallel pervious layers of infinite extent comparing the multilayer results to two different equivalent models, single layer and sandwich model. Another issue raised by this layer geometry is the connectivity between layers. Flow-log data show that in general the layer distributions in two wells of a doublet do not correspond (Hamm et al., 2015) (different layer number, different thickness and flowrate distributions (Figure 2(a)). This observation leads to suppose that in some cases the hydraulic connection between the two wells may be established by two connected layers, each one intercepting a single well. The probability of such a scenario is expected to increase when the interbedded aquitards become semi-pervious. At last, though the incorporation of the connectivity concept in an equivalent model is a complex task, the streamtube model used by G&S in their model may be of help to model temperature transport as a channeling process from one doublet well to the other through different layers.

We revisit here the equivalent model issue by means of numerical simulation and the G&S model, and its variants exposed previously (§2). The numerical code is the reservoir flow simulator Pumaflow developed by BeicipFranlab for petroleum and geothermal engineering applications (https://www.beicip.com/software/pumaflow/).

3.1 Sandwich distribution

We consider two sandwich models, the first one with a fixed thickness of the three layers system (h+e) and different combinations of the pervious and impervious layer thicknesses, h and e respectively, and the second one with different thickness values of the system but a fixed pervious layer thickness i.e. with a varying aquitard thickness. In both models the two cases, with and without burdens, are considered. The objective is twofold: 1) understand the respective importance of the interbedded aquitard and the burden on the evolution of the production temperature, and 2) verify if the proposed equivalent model behaves as expected when the geometry of the sandwich distribution change. In the first model the total thickness is e+h = 18.4 m. and the combinations of the pervious and impervious layer thicknesses (in m.) are (e, h) = (2×1., 16.4), (2×2., 14.4), (2×4., 10.4), (2×6., 6.4), (2×8, 2.4). In the second model the thickness of the two pervious layers is e = 2 × 4.5 m., and the total thickness values (in m.) are (e+h = 10., 14., 23., 27.) The different physical rock, fluid and flow parameters are given in table 1.

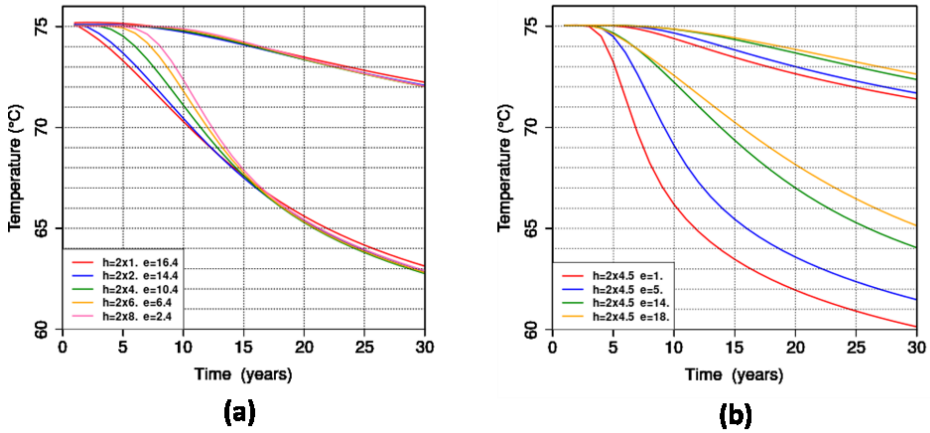

Figure 4: Temperature evolution in the production well for the different configurations of the first (a) and second (b) sandwich models respectively. The upper curves take the burdens into account and the lower curves neglect them.

Figures 4(a) and 4(b) display the temperature evolution in the production well over 30 years for the different configurations of the first and second sandwich models respectively. In both models the curves with no burdens are decreasing much more rapidly than with burdens, which is expected. In the first sandwich model, where the total thickness is fixed, the five production temperatures merge towards a single curve. When the burdens are present this convergence takes place immediately, and when they are not it takes approximatively 15 years. Figure 5(b) shows that the G&S monolayer model gives a temperature curve very close to the bundle of curves. These results show that 1) the temperature does not depend on the layers combination, and 2) the impervious layer does not play any role in the production curve. This not the case for the second sandwich model. Figure 4(b) shows that, for a given pervious layer thickness, the temperature decay becomes less pronounced as the impervious layer thickness increases, and this, with and without burdens. As expected the breakthrough time increases when the pervious layer thickness decreases.

These observations lead us to suppose that in both models the temperature evolution depends principally on the thickness of the three layers. If we suppose that the characteristic thermal transfer time τ (Equation 5) is much smaller than the travel time t_a, whatever the streamline, equation 6 may apply. According to §2.2 this equation holds at the the zeroth order in $\varepsilon = \tau/t_a$, which means that the pervious and impervious layers are in thermal equilibrium layer at any time. An estimation of τ is given by the relationship $(e + h/2)^2 = 4D_r\tau$, where D_r is the rock thermal diffusivity. With the thickness values considered in the sandwich model the characteristic time does not exceed one year, which is smaller than the travel times observed in the simulations or computed with the dipole model (§2.1). Figures 5(a) and 5(b) display the simulation results for the different configurations of the first and second sandwich models respectively, the solutions of the effective equation 6 for both cases, burdens and no burdens, and also the exact solution of Carslaw and Jaeger (Carslaw and Jaeger, 1959) when the burdens are neglected. When the burdens are present the effective approach provides a solution quite close to the simulation results. When burdens are neglected the exact solution of Carslaw and Jaeger is quite different. Whatever the model this exact solution decreases more rapidly than the simulated one after the arrival time and then decreases at the same rate. If the arrival times are more or less the same, the temperature at 30 years differ by two degrees. We believe that the code numerical and physical dispersion, which is absent of the model of Carslaw and Jaeger, is the source of these differences. We also observe that the solution of the effective equation behaves as expected. This effective equation, which is not given here, is the equation 6 with an additional diffusive term coming from the homogeneization process (expansion in powers of $\varepsilon = \tau/t_a$).

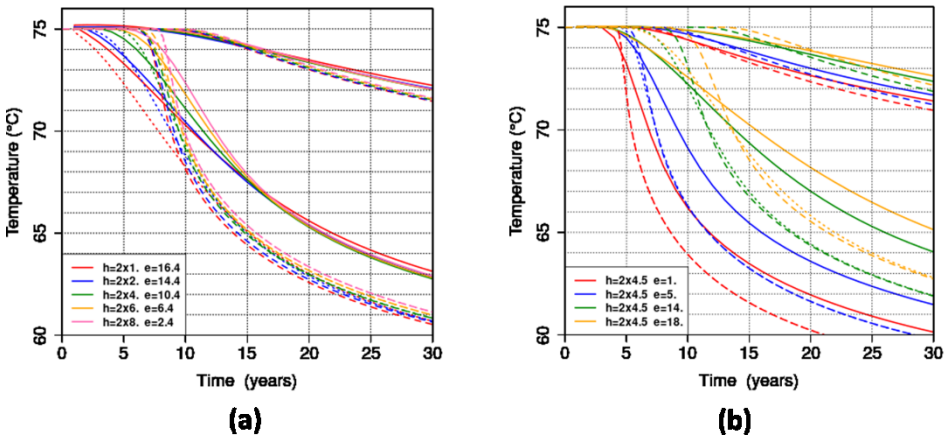

Figure 5: Simulated (solid line) and modeled (dashed line) temperature evolutions in the production well for the different configurations of the first (a) and second (b) sandwich model. When burdens are neglected the dashed line represent the simulation with the effective equation and the dotted line the exact solution of Carslaw and Jaeger.

3.2 Disk distribution

The pervious layers are now considered as elliptical disks of finite lateral extent and distributed in the Dogger reservoir model of the Ile de France region following the Object Modeling algorithm of Petrel©. The reservoir is made up of three depositional environments: Upper Offshore, Shoal/Shoreface and Lagoon (Figure 6). The disks represent the low cemented facies of the reservoir. The horizontal distribution of the disks is random and the vertical one is conditioned at the wells. The disks dimensions are distributed randomly in space and follow a gaussian distribution with a mean characteristic dimension of 1000 m. The reservoir model is made up of 90 layers and contains 1018980 cells (100m.×100m.×1-10m.). On the basis of the standard facies model three models of increasing petrophysical heterogeneity have been constructed (Figure 6). Model 1 is Boolean; the pervious disks are embedded into a homogeneous impervious rock matrix (*i.e.* the three depositional environments). In model 2 the three depositional environments are distinct and homogeneous. The disks are less pervious than in model 1. In model 3, the petrophysical properties of both depositional environments and disks are heterogeneous and distributed log-normally. The geothermal doublet is the Alfortville doublet (Table 1). The number of productive layer (disks) intersecting the injection well is 7 and the production well 6 (Figure 2b). Finally, ten geostatistical realizations of the disk distribution are generated and inserted in each of the three geological models.

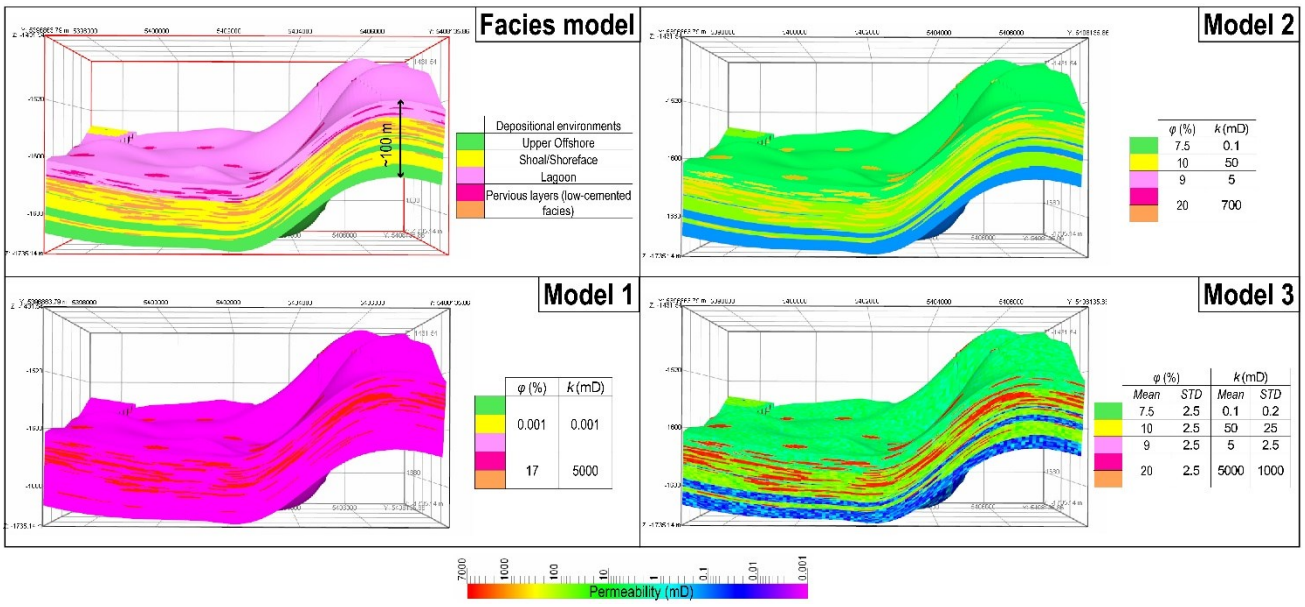

Figure 6: Standard Facies model of the Dogger reservoir and models of increasing petrophysical heterogeneity (porosity φ and hydraulic conductivity k) based on the standard model.

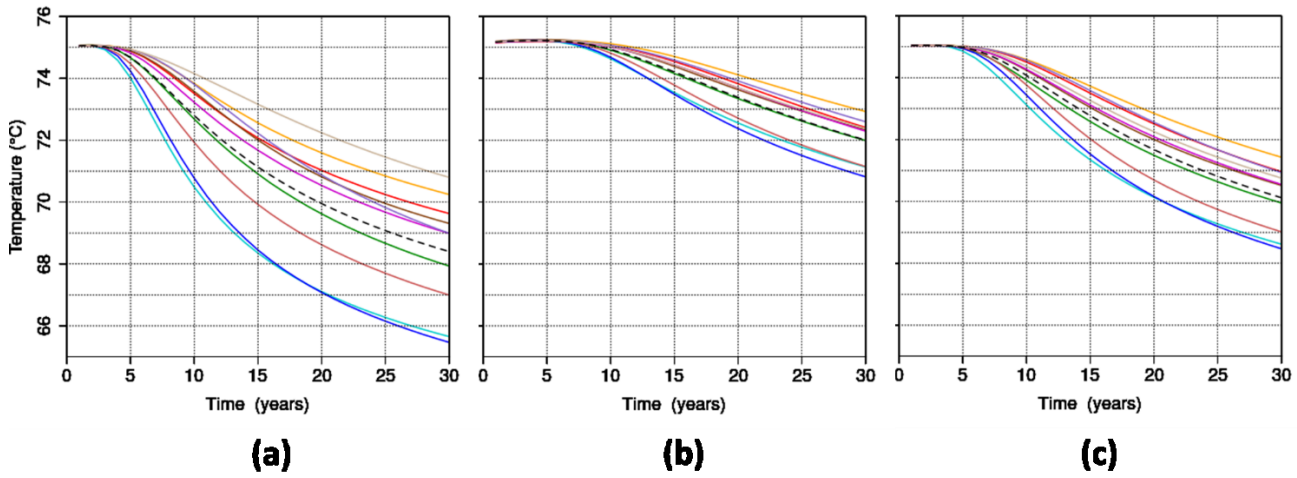

Figure 7: Simulated temperature evolution in the production well for the ten disk realizations and the three models (model 1=(a), model 2=(b), model 3=(c)). The dashed black line is the mean temperature evolution.

Figures 7(a), 7(b) and 7(c) display the simulated temperature evolutions in the production well over 30 years for the ten disks realizations and the three models. In model 1, the Boolean model, we observe that the temperature range at thirty years extends over six degrees and the lowest temperature is below 66°C. This temperature is lower than the temperature given by the G&S model with the same nominal pervious layer thickness and a flowrate twice greater (Figure 2(b)). The arrival time is smaller than 5 years. In model 2 the dispersion of temperatures is lower than in model 1, two degrees at thirty years, and the arrival times lie in the range 7-10 years. Model 3 shows an intermediate comportment.

The analysis of the vertical cuts of model 1 passing through the wells show a strong correlation between the disk connectivity and the production temperature. When the wells are connected "directly" through the disks, because of disk connectivity, the temperature decrease rapidly with time, and when this is not the case the decrease is much slower. In our case, the mean disk diameter (1000 m.) is nearly equal to the inter-well distance (1300m.), and the disk density is conditioned on the flow logs at the wells. For these reasons the wells are always connected and the question is how direct is this connection? Roughly, if the connected pathway is located inside the inter-well circle (Figure 3(a)) the connection is qualified as "direct". If it is outside the connection is "indirect". Figure 8 illustrates this connectivity issue. Figure 8(a) displays a direct connection between the two wells and the temperature plume moves rapidly along the pathway. When this "direct" connection does not exist (Figure 8(b)) the plume moves more slowly along a "nondirect" pathway. These two cases, connected and non-connected, are associated respectively to the upper and lower temperature production temperature curves of model 1 (Figure 7(a)).

In model 2 the hydraulic conductivity of the depositional environments is non-zero and flow can take place, even if the conductivity contrast with the disks is of one or two orders of magnitude. For this reason, the flow channeling is less pronounced than in Model 1. We believe that the connection of disks through the shoal/shoreface environment (Figure 8(b)), which conductivity is just one order of magnitude lower (k=50 mD, Figure 6), is efficient enough to consider that the wells are connected through an equivalent pervious layer. This probably explains why the mean production temperature (dotted curve in Figure 7(b)) is almost identical to the bundle of temperature curves describing model 2 of the sandwich distribution (Figure 4(b)). Model 3 is Model 2 with sub-scale heterogeneities in each facies unit. We believe that these heterogeneities produce sub-scale channels percolating throughout the whole inter-well domain. It probably explains why this model leads to an intermediate thermal comportment. At last, the mean production temperature evolutions plotted on figures 7 should be interpreted with a G&S model including a dispersion term, to take account for the statistical variability of the pathways. Including a dispersion process has been done in single fracture transport models (Tang et al., 1981) but the solution is highly complex and is not proven to converge to the G&S solution when diffusion in the fracture tends to zero. This issue is unfortunately a limitation to the use of G&S model.

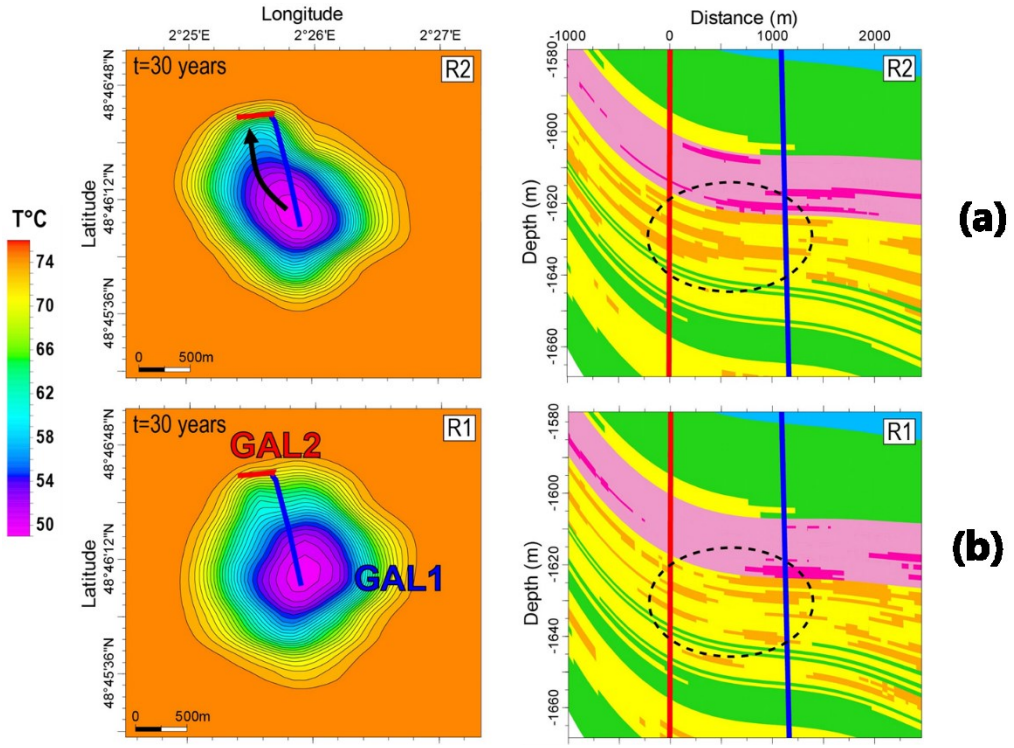

Figure 8: Temperature lateral distribution at 30 years and vertical cross section including the injection well (GAL1), in blue, and the production well (GAL2), in red. The cross sections show the facies distribution and the pervious disks in orange. Figure 8(a) and 8(b) display respectively a connected case and a disconnected one.

4. CONCLUSION

We showed that the model developed by Gringarten an Sauty in 1975 is of valuable help to understand the geothermal comportment of a doublet in a multilayered reservoir. This model is simple enough to manipulate, both from a theoretical and a numerical point of view, and also to produce model variants adapted to specific situations (multilayering, presence or not of burdens, channels, …).

In the sandwich model, similar to the dual porosity model used in reservoir engineering or hydrogeology, we propose to replace the model by an equivalent monolayer model. This can to explain qualitatively simulation results. Nevertheless, from a quantitative point of view, the production temperatures given by each of the two models are significantly different. We believe that the absence, in the G&S model, of thermal diffusion in the transport through the pervious layer could explain these differences.

In the geostatistical case of 3D disk distribution, again, the G&S model has proven to be a valuable tool to understand how production temperature may be governed by connectivity and channeling. The inclusion of a flowrate angular distribution to simulate channels in the G&S model is under work (Mouche et al., in prep.). The next step would be to add in the toolbox a particle tracking code to analyze the temperature transport pathways in a heterogeneous reservoir and apply the G&S methodology to each streamline. This would require to work on a refined mesh to obtain precise particle statistics.

Aknowledgments

This work is supported by the UPGEO program “Upscaling and heat simulations for improving the efficiency of deep GEOthermal energy”. The program is funded by the Agence Nationale de la Recherche [referenced ANR-19-CE05-0032-01]

REFERENCES

Antics, M., Papachristou, M. and Ungemach, P.: Sustainable heat mining. A reservoir engineering approach, Proceedings, 30th Workshop on Geothermal Reservoir Engineering, Stanford University, Stanford, CA (2005).

Barker J.A.: Modelling doublets and double porosity, Quarterly Journal of Engineering Geology and Hydrogeology, 43, (2010) , 259-268.

Carslaw H.S. and Jaeger J.C.: Conduction of heat in solids, Clarendon Press (1950).

Catinat, M., Fleury, M., Brigaud, B., Antics, A. and Ungemach, P.: Estimating permeability in a limestone geothermal reservoir from NMR laboratory experiments. Geothermics 111, (2023a), 102707.

Catinat, M., Brigaud, B., Fleury, M., Thomas, H., Antics A. and Ungemach, P.: Characterizing facies and porosity-permeability heterogeneity in a geothermal carbonate reservoir with the use of NMR-wireline logging data, Geothermics 155, (2023b), 102821.

Catinat, M.: Caractérisation multi-échelle des hétérogénéités du réservoir géothermique du Dogger d'Ile-de-France: apport de la résonance magnétique nucléaire et de la modélisation numérique statique et hydrodynamique, (2023c), Doctoral Dissertation, Université Paris-Saclay.

Gringarten, A. C. and Sauty, J. P.: A theoretical study of heat extraction from aquifers with uniform regional flow. Journal of Geophysical Research, 80(35), (1975), 4956-4962.

Guo, B., Fu, P., Hao, Y., Peters, C. A., and Carrigan, C. R.: Thermal drawdown-induced flow channeling in a single fracture in EGS. Geothermics, 61, (2016), 46-62.

Haggerty, R. and Gorelick, S. M.: Multiple-rate mass transfer for modeling diffusion and surface reactions in media with pore-scale heterogeneity. Water Resources Research, 31(10), (1995), 2383-2400.

Hamm, V., Treil, J. and Receveur, M.: Gestion du Dogger et corrélations entre niveaux producteurs,. Final Report N° BRGM/RP-65472-FR, (2015). BRGM, Orléans.

King, P. R.: The connectivity and conductivity of overlapping sandbodies,, North Sea Oil and Gas Reservoirs-II, Graham and Trotman, London, (1990), 353-361.

Lauwerier, H. A.: The transport of heat in an oil layer caused by the injection of hot fluid: Applied Scientific Research, Section A 5, (1955), 145-150.

Lebrun, M., Hamm V., Lopez S., Ungemach P., Antics M., Ausseur J.Y., Cordier E., Giuglaris E., Goblet P and Lalos P.: Hydraulic and thermal impact modelling at the scale of the geothermal heating doublet in the Paris Basin, France. Proceedings 36th Stanford Geothermal Workshop., Stanford University, Stanford, CA (2011).

Lopez, S., Hamm, V., Le Brun, M., Schaper, L., Boissier, F., Cotiche, C. and Giuglaris, E.: 40 years of Dogger aquifer management in Ile-de-France, Paris Basin, France. Geothermics 39, (2010), 339–356.

Sudicky, E. A., and E. O. Frind. Contaminant transport in fractured porous media: Analytical solutions for a system of parallel fractures. Water Resources Research, 18(6), (1982): 1634-1642.

Tang, D. H., Frind, E. O. and Sudicky, E. A.: Contaminant transport in fractured porous media: Analytical solution for a single fracture. Water resources research, 17(3), (1981), 555-564.

Tsang, Y. W. and Tsang, C. F.: Flow channeling in a single fracture as a two-dimensional strongly heterogeneous permeable medium. *Water Resources Research*, *25*(9), (1989) 2076-2080.

Thomas, H., Brigaud, B., Blaise, T., Zordan, E., Zeyen, H., Catinat, M., Andrieu, S., Mouche, E., Fleury, M.: Upscaling of geological properties in a world-class carbonate geothermal system in France: From core scale to 3D regional reservoir dimensions. Geothermics 112, (2023), 102719.